Contents

Highlights

Some of the surface states of gold vicinal surface within density functional theory

Chureh Atasi, Oleksandr Motornyi, Andrea Dal Corso, Nathalie Vast

- November 12, 2023
- Introduction
- Computational method
- Results
- Conclusions
- Appendices
- Bibliography

Some of the surface states of gold vicinal surface within density functional theory

Chureh Atasi[a,b], Oleksandr Motornyi[a], Andrea Dal Corso[a], Nathalie Vast[a]

[a] *Laboratoire des Solides Irradiés, École Polytechnique, CEA/DRF/IRAMIS, CNRS UMR 7642, Institut Polytechnique de Paris, 28 Route de Saclay, F-91128, Palaiseau Cedex, France*

[b] *Georgia Tech(maybe)*

Abstract

Abstract goes here

Keywords:
vicinal surface, surface states, gold surface, plasmons

1. Introduction

Noble metals, specifically gold, exhibit very useful and clear surface states on their Vicinal surfaces. Vicinal surfaces naturally assemble in an ordered array of nanostructures [1-6] and house-tailored electronics surface states, whose spin and energy properties can be characterized through DFT computed band structures. The coupling between light and plasmons localized on a surface gives rise to an excitation of an electromagnetic field (EMF) by several orders of magnitude near a metallic surface. Such plasmon-polariton excitation is made possible by the grating of the planar metal surface. The concentration of the EMF with micrometer-scale grated gold surfaces (MSGS) are of interest for surface-enhanced Raman scattering (SERS), e.g.[Mubee:2012], but MSGS plays a role in a wealth of technological applications, like surface plasmon resonance biosensors, near-field imaging, and plasmonic wave-guide Y-splitters, to name a few [Holmgaard:2008]. Because of their atomic steps, vicinal surfaces of gold can be seen as surface grating on the atomic scale which would potentially decrease the size of plasmonic devices. However, surface states on vicinal surfaces have been theoretically

Email addresses: chureh.atasi@gmail.com (Chureh Atasi), nathalie.vast@polytechnique.edu (Nathalie Vast)

less studied than in experiments.W[1].

Au (111) surfaces have been heavily studied in the past [6-12], with both DFT and experimental results, exhibiting similar values. Experimentally, gold surfaces, provide us with the clearest view of surface states. These states are called Shockley states [Fortzmann and Shockley], arise from the breaking of the periodic boundary condition. We demonstrate this rise of states with a simple yet effective matrix experiment. However, these 111 surfaces tend to form many reconstructions [PHYS Rev B 43:17, Takeuchu], which are hard to model theoretically as the herringbone reconstruction is not truly accurate for the 111 surfaces. Hence The flat surfaces are hard to simulate, unlike the vicinal surfaces, which experience little reconstruction as they form naturally in nanostructures. These surfaces are simply stepped surfaces, that are characterized by a step width and size. Using readily found libraries, one can simulate these values and create a unit cell that possesses the required properties. This unerring similarity between experiments and theoretical slabs is what motivates us to perform this research. We model the vicinal surfaces (322, 455, 788) using quantum espresso and thermo_pw [dal_corso].In this paper, we discuss our methods of how characterizing the electronic structure of the vicinal 111 surfaces within Fully relativistic approximations. We also include a spin study of these surfaces and demonstrate the presence/lack of Rashba splitting [Lobo Checa PRL 104 2010]. Calculation on vicinal the surface has not been done from the first principles, and so we shall compare our results with their experimental counterparts and draw deductions. This paper is constructed as follows: II. Computational methods that cover the model, band structure, assignment of Shockley states, characterization of energy dispersion, III results for the (322 455 788) surfaces, III Discussion where the spin structure and effective mass models are discussed, and IV. Conclusion.

2. Computational Methods and Theory

2.1: DFT Setting to compute the electronic structure:

In our calculations, we have chosen to perform a Fully relativistic (FR) approximation of the Dirac equation. We note that this is significant, as we desire quantitative results rather than pure qualitative ones. Fully relativistic effects become more predominant in elements with larger masses such as gold, as electrons in the outer shell have higher momentum than electrons in

the lighter elements. We have chosen the Generalized Gradient Approximation pseudo-potential or Perdew–Burke-Ernzerhof (PBE). We have chosen this functional over LDA, as we are interested in passivating our surface by reducing the number of layers in a cell by. This can be achieved by inserting a hydrogen layer on any surface. Since one surface has no states, then this would avoid any hybridization or lifting of the degeneracy. Not accounting for any hybridization effects certainly lets us reduce the number of layers required for true convergence. We note that the difference in energies of the eigenvalues in the (111) surface FR between LDA and GGA is 0.018 eV at the equilibrium lattice parameter of 7.71 a.u. for Gold FCC. Since DFT is a variational theorem at the core of it, we must try to obtain the smallest number possible (minimum). Within the GGA J. P. Perdew, K. Burke, and M. Ernzerhof, approach for the exchange-correlation calculations, we have obtained an error of about 10^{-3} eV for bulk Au. This corresponds to energy ecutoff= 40 Ry, and a 16 16 16 monkhorst-pack k-point mesh with a degauss value of 0.02 Ry. The error values increase slightly as we move towards more complex systems. i.e. vicinal surfaces.

2.2: Geometry of the vicinal surface:

A. In the real Space

When simulating these surfaces, we must take into account the geometry or crystallographic orientation of the gold surfaces, along with the vacuum. These together can model the surface-vacuum system. We construct a gold slab that is essentially a super-cell made from gold atoms- in a certain arrangement- and vacuum (No atoms). Like this, we mimic the breaking of the periodic boundary conditions which are at the core of all surface states. Our slab constitutes an n-layer of gold atoms where, followed by an p-layer of vacuum, followed by an n-layer of gold, and so on. This slab-vacuum system is out of the surface. We take a number of the layers that are in close proximity to the vacuum and we name the "surface layers". We calculate the density of electronic states on these surface layers

Of course, this model has its limitations. First and foremost, the surface states- if extended well into the bulk of the slab- could hybridize with the opposing surface state. Hence, two states that are ideally degenerate in their energy levels, are shifted by some minuscule energy eV. This is affected mainly by the number of layers in each slab. The thicker the slab the less likely that the surface states will propagate all the way through to the end. This makes the calculation more expensive, however. Secondly, this model

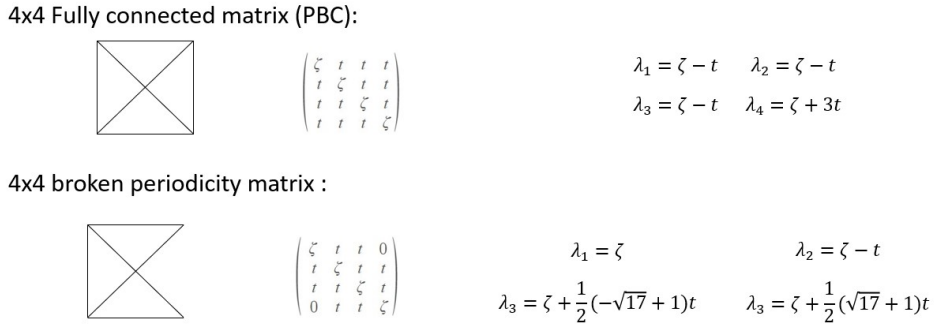

Figure (1) Shockley state explanation

in its primitive form does include any surface reconstruction, which is what usually happens in experiments. However, that depends on the surface itself. For instance Au(111) see heavy reconstruction [Sietsonen surf sci 643, Ishida 2022 J. Phys.: Condens. Matter 34 195002]. There are methods to simulate said reconstruction in DFT calculations, but they are all approximations and do not necessarily represent the experimental truth.

Since all our surfaces are vicinal with respect to the Au (111) surface, we shall start by characterizing the latter surface. In its equilibrium states gold exhibits a face-centered cubic Bravais lattice. When we project the FCC Brillouin zone in the [111] direction, we obtain a rhombohedral (trigonal) shape. As seen in the figure below. Hence like this, we can simulate our surfaces as layers of hexagonal shapes. Our optical surface the Au(111) happens to be coinciding with the actual physical surface. But that does not have to be the case, as we will see in the vicinal surfaces.

Vicinal surfaces are described in the image below. They contain an array of stepped structures with defined width L, height h, angle $\alpha = \arctan h/L$. Note that setting $L \to \infty$ gives us back the flat 111 surface. These surfaces are characterized by their optical surfaces, the surface that corresponds to rotational angle α with respect to the flat Au(111) surface. Here we see that the optical surface does not necessarily align with the actual surface but contains all the necessary information to describe the vicinal surface.

B. In the Reciprocal Space

We saw that the Au(111) surface can be modeled with the hexagonal Bravais lattice through the Bain path [6]. An FCC Bravais lattice can be modeled

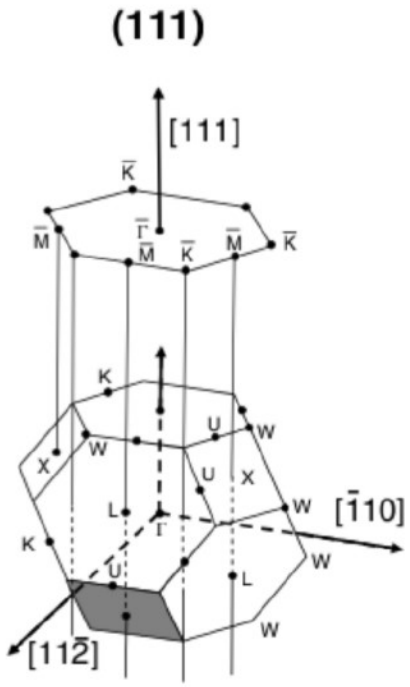

Figure (2) hexagonal 111 surface

perfectly by a rhombohedral cell with characteristic angle $\alpha = 60$. However, this unit cell does not provide us with the needed Surface Brillouin Zone (SBZ). To convert that to a hexagonal cell we must divide the primary lattice parameter a by $\sqrt{2}$ and have the second lattice parameter $c = \sqrt{2}$. Like this, we project the FCC cell into the Au (111) surface. This is the smallest Wigner-Seitz unit cell possible for such a configuration. Because our hexagonal lattice happens to account for exactly the number of atoms in the actual surface, no band refolding is observed.

In the case of vicinal surfaces, the smallest Wigner-Seitz unit cell needed to describe the system must be an orthorhombic cell. Because of the bumps in the optical surface, we must use a bigger Wigner-Seitz unit cell. This means that the reciprocal Bravais lattice vectors are now reduced, which in effect cause refolding, as we need more and more vectors to describe the same state. A vicinal surface of Au(111) consists of flat (111) terraces separated with monoatomic steps and has the orthorhombic unit cell with the

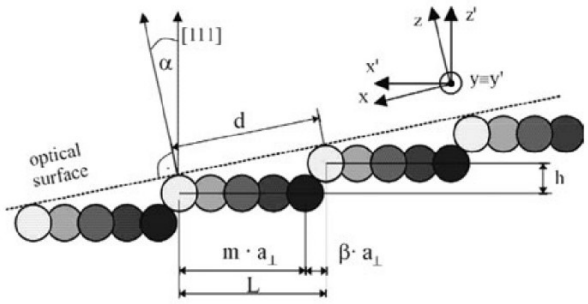

Figure (3) vicinal surfaces in real space

rectangular SBZ.

If we use the orthorhombic cell to model the 111 surfaces, we can implement a method to unfold the bands. This unfolding manipulates the system's symmetry to erase redundancies [Motoriny] bandUP code [77, 78]. However since this symmetry does not exist in our vicinal surface unit cells, we cannot use the BandUP code. This procedure is not as straightforward for the vicinal surfaces due to the refolding of the band structure of the vicinal surfaces that complicates the obtainment of the PBS and band structure as well as the precise location of the localized states in the PBS gaps.

Furthermore, we have two different types of steps 100 and 111 depending on how we measure the cut [4].

2.3: Band Structure Refolding and Direct Calculation:

DFT calculations permit us to study the projected band structures and differentiate surface states from resonance states [2]. The projected band structure is the bulk electrons' bands being grouped and cast on the SBZ. Hence this projection essentially includes the bands of the bulk electrons when they are projected onto the surface (Appendix 3). Figure 2 helps us visualize this effect. Since these projections are simply FCC bands being projected onto the hexagonal cell, then we can observe the bulk band structures and see how these projections and gaps arise. Looking at figure 4.

The L point is projected onto the Gamma point as we see in figure 2. Hence we can define the L gap in figure 4(a) as the space left untouched when the L point is projected onto the Γ k-point. Hence Shockley states

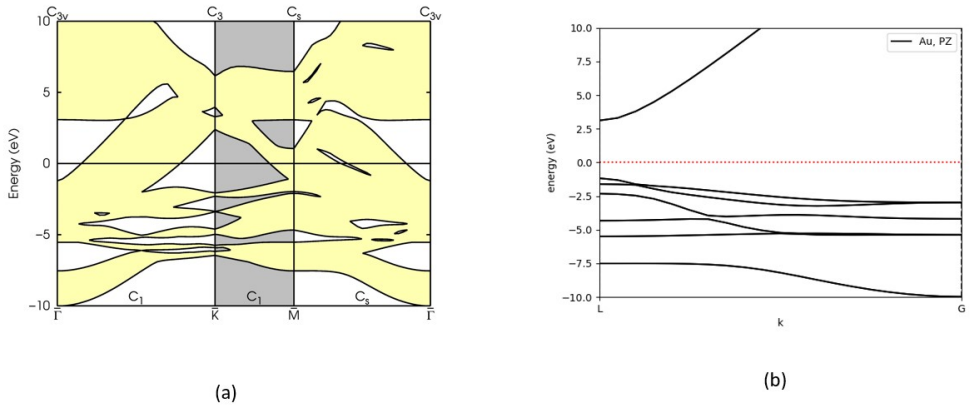

Figure (4) Here we compare the projected bulk band structure with the normal bulk band structure of Gold FCC

found on the Au(111) surface are said to be true surface states as they lie in the band gap of the PBS, called L-gap, in this case, [5]. In order to identify whether a Shockley state is a true or resonance state in our vicinal surfaces, we must perform this bulk band calculation for each surface. Since each stepped surface is defined by an optical surface rotated at an angle θ with respect to the [111] vector- in any direction- then we can define a function that relates the angle to an L-gap open under the Fermi level. This is seen in Figure 5.

Most significantly, we notice that the Au (322) surface lies in the negative PBS region, meaning the gap begins above the Fermi level in this vicinal surface. Therefore, no occupied true surface states occur in the Au(322) surface, only resonances that hybridize with the bulk bands. We note that a gap exists under the Fermi level for Au 455 and 788. We shall continue to define the surface states in 322, as these states are still quite pronounced in experimental results [3].

2.4: Assignment of a State to Shockley's State

In order to identify Shokley's states, we must locate them on the surface. This implies that it should have a high probability value of being found near the surface. This is done by defining a surface length and position and then integrating the wave function over that displacement. If it's higher than a certain threshold then we set it as a surface state. Clearly, if a state hybridizes with the bulk, then it will have a higher probability to be found

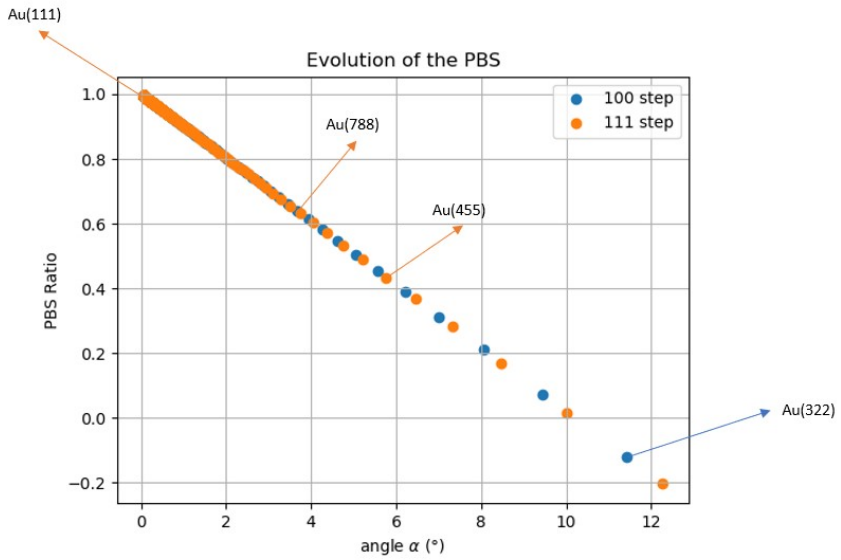

Figure (5) Expected gap in the PBS under the Fermi level vs the angle of the optical surface. We have noted the interesting surfaces for this paper

in the bulk, hence a smaller value will be assigned for the threshold. The states we are most interested in, are the occupied states, i.e. below the Fermi level. These states are likely to form surface plasmonic excitation, which is the main aim of this research. (Details Appendix 4)

2.5: Characterization of energy dispersion of a surface state

In many of these states, we will study the band structures of gold and try to model them using the Kronig-Penny function. Since our surface consists of a regular array of steps, then we could model this system with the KP model. Let d be the spacing between each step, then we can model the potential energy as a sum of delta functions.

$$V_{KP}(y) = U_0 b \sum_{i=0}^{\infty} \delta(y - di) \tag{1}$$

Note that this is different from a flat surface or free electron model where $d = \infty$. In the flat surface case, we assume the electron is in an unrestricted potential with an effective mass m^*. In vicinal surfaces, however, this ap-

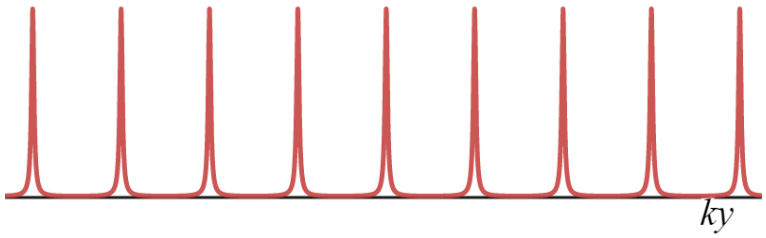

Figure (6) The potential of the Kronig penny can be modeled as a series of delta functions

proximation does not hold very well, due to the existence of steps. The potential of such steps could be modeled with Eq (1) as seen above. Solving the Schrodinger Equation with V_{KP} provides us with the following energy Eigenvalue.

$$E_{KP}(k_y) = E_0 + \frac{\hbar^2}{2m^*}\frac{1}{d^2}[\arccos(|T|\cos(k_y d)) - \phi]^2 \tag{2}$$

Where

$$|T|^2 = \frac{1}{1 + (q_0/q)^2} \qquad \phi = -\arctan(q_0/q)$$

$$q_0 = \frac{m^*}{\hbar^2} \cdot U_0 b \qquad q = \sqrt{\frac{2m*}{\hbar^2}(E - E_0)}$$

Note that Eq.(2) reduces to $\frac{\hbar^2 k_y}{2m^*}$ when $d = \infty$, just as we would expect from the behavior of a step energy eigenvalue. This occurs because the Transmission coefficient $|T| \to 1$ as $q \to 0$. A more interesting limiting factor, however, occurs on the other side of the spectrum. Assume we set the boundary conditions $U_0 b \to \infty$. We can see that this is caused by $|T| \to 0$ and $\phi \to -\pi/2$ as $q_0 \to \infty$. Because of the term, we see a quantization of our energy eigenvalues, where for any integer number:

$$E_\infty = E_0 + \frac{(\pi\hbar)^2}{2m^* d} N \tag{3}$$

This is nothing but the infinite barrier model of quantum mechanics. Hence the KP model fits well into both limits of a free and bound electron. We will see how these limits are reached within our different surfaces. For each surface, we can calculate the effective mass $m*$ and the corresponding delta function coefficient $U_0 b$.

2.6: Characterization of the wave function of a surface state

These electronic states exist in 3D space, and thus have a wave function in all directions. In the direction perpendicular to the surfaces, these surface states are characterized by an exponential decay and cosine function. We see this in the flat 111 surface as well as the vicinal surface. wave-function on the surface however differs greatly. On a flat surface, we model the system as an electron in an unbound potential. Hence it has a continuous plane wave characterized by wave-number $\vec{k}$. This is true in both the $\hat{x}$ and $\hat{y}$, as the flat surface extends infinitely in both directions. In the vicinal, on the other hand, we observe this continuous plane wave only in the $\hat{x}$ flat direction. The $\hat{y}$ (perpendicular to the surface) direction experiences a non-zero potential, specifically, a Kronig-Penny potential. This alters the wave function in the direction perpendicular to the steps. The wave functions that are formed depend on the step size and hence the $U_0 b$ value. Because of this, there exist two different modes for the wave function perpendicular to the surface, namely, Terrace modulated and surface modulated. The wave function can be localized within a certain "grate" or terrace of a step. This occurs when the step is big enough to act as an infinite barrier. Here we see multiple wave functions all localized within the surface grating, with little transient states leaking across. Once the step size becomes smaller, the potentials get weaker, and hence we can observe the wave function extending over the entire surface, analogous to a flat surface, but with fewer uniform

amplitudes, due to the presence of grating. These are referred to as average modulated wave functions.

This difference between the two alters the wave function in the $\hat{z}$ direction. We still observe an exponentially decaying cosine function but with different frequencies. We can think of this as the wave function being shifted by an angle α of from the [111] direction. This causes the frequency to decrease. The equation to describe these wave functions is given by:

$$\psi(z) = A_i e^{kz} \cos\left(\frac{G_m z}{2} + \delta\right) \tag{4}$$

Where $G_m = \frac{2\pi}{a}\cos(\alpha)$ at a distance a between the consequent layers. Not that when the α is 0, corresponding to a flat surface, we simply retain the periodicity of the lattice of stacked layers. We note, however, that a larger $U_0 b$ value that corresponds to terraces modulated wavefunction, has a smaller angle and thus G_m value deviation. We can think of this as the higher the miller indices the closer the system is to the (111) surface in terms of the angle of deviation α.

To summarize some of the surface information, we present the table below. It characterizes the geometry of the surface.

Surface	miscut angle	Terrace Width $\mathring{A}$	Gap at E_F	$G_m/2, \mathrm{a\,u}^{-1}$
Au(111)	0°	∞	Yes	0.706
Au(322)	11.4°	12	No	0.692
Au(455)	5.76°	23.3	Yes	0.702
Au(788)	3.51°	38.3	Yes	0.7045

3. Results for vicinal surfaces

3.1: Au (322) Vicinal Surface

We start with Au(322) as it has the smallest number of atoms per cell. In Figure 7, I plot the band structure of Au(322) from the $\bar{Y}$ to $\bar{\Gamma}$ k-point. I demonstrate my results in comparison with experimental results. As you can see in the figure I draw two orange lines that encapsulate the surface states that have a localization on the surface of $|\psi|^2 > 0.38$. This is a rather low number but it can be explained by Figure (5).

As we know Au(322) has a miscut angle of $\alpha = 11.4°$, which according to Figure 15, says that the PBS covers the surface states. In other words, the

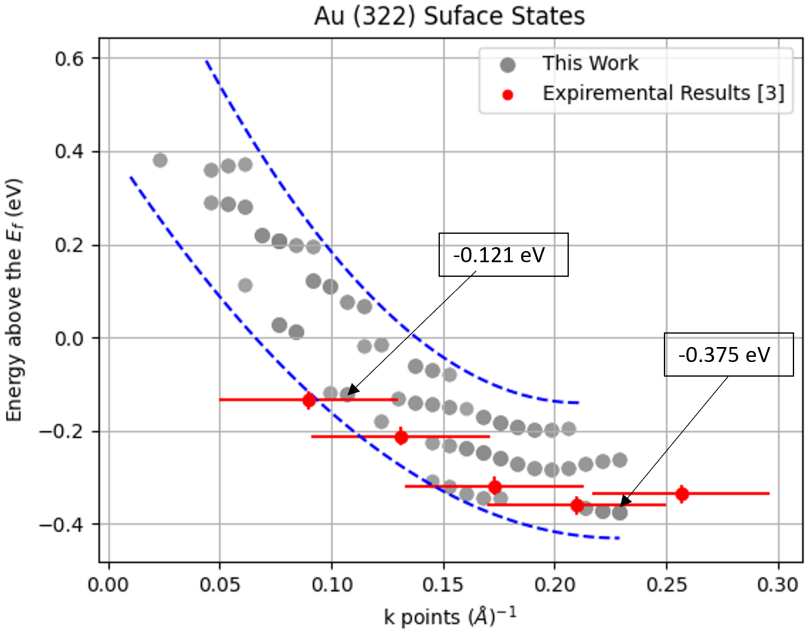

Figure (7) The dispersion of the Au(322) surface state, from $\bar{Y}$ to $\bar{\Gamma}$ k-point. Grey dots mark the states identified as partially localized, the bolder the more strongly localized, and the red symbols mark the experimental results [35] Arrows mark the surface states for which planar averages are shown in Fig. 5.10. The Au(322) surface was modeled with a 105 atom slab (50 Å thickness)

surface states do not lie in the L Projected Band Gap. This phenomenon gives rise to two consequences: (1) The state is less localized on the surface as it hybridizes with the bulk state. (2) There exists a mix of bulk and surface states with this criteria. A phenomenon we refer to as surface resonances. Hence here we define a "Window" where surface resonances can be found, calculated, or measured. The tentative edges of the energy window for this surface resonance are marked with blue dashed lines. Experimental results obtained using ARPES fall very close to our window. Note that if we compare the minimum energies at $0.21\mathring{A}$ we find a very small difference between the most localized point of our calculation and the Experimental value. $\Delta E_{DFT-Exp} = 0.0422\ eV$. Hence if we trace out our bands from the minima, then we get very similar results. In other words, our most localized surface resonance lies very close to the experimental results. Furthermore, we can see that the shape, and thus the effective mass, of the calculated dispersion of the Au(322) surface resonance is in good agreement with the dispersion measured experimentally.

Now let us concentrate on the character of this surface resonance, specifically on the planar averages of the charge density and charge density distribution with respect to the step. In Fig. (8) I plot the planar averages for three states at the minimum energy at $\bar{Y}$ K-point, and at another K-points close to the Fermi level (marked with arrows in Fig. 7). These states show a behavior typical of a surface resonance: they are partially localized within 10 a.u. around the surface and they extend infinitely into the bulk. These states cannot be fitted into closed-form functions such as Eq(4), as these states do not exhibit single-mode frequency oscillations. A Fourier series of oscillatory functions could be used to model these random fluctuations. The components of the Fourier series will be a combination of both the bulk and surface states, as expected from the surface resonances.

In our final step of analysis, we attempt to fit the Kronig-Penney model into our surface states. Our stepped surface provide the potential energy depicted by Figure (6). Hence our surface can be fit with Eq(2). The KP energy eigenvalue equation is inherently a recursive function and is heavily dependant on E_0 the minimum energy. Hence I fit the bend that stems out from the most strongly localized minima at the $\bar{Y}$ K-point. This point minima is depicted by the arrow in figure (7). I perform the fit as depicted in Figure (9)

We estimate the step barrier strength from the results of this fitting. We get a value $U_0 b = 1.06$ eV and the effective mass $m^* = 0.24 m_e$ obtained from the parabolic fit of the bands in the y direction (along the $\bar{Y}$ - $\bar{\Gamma}$ path). Note that our KP fit plots and that of the free electron fit are very similar. This

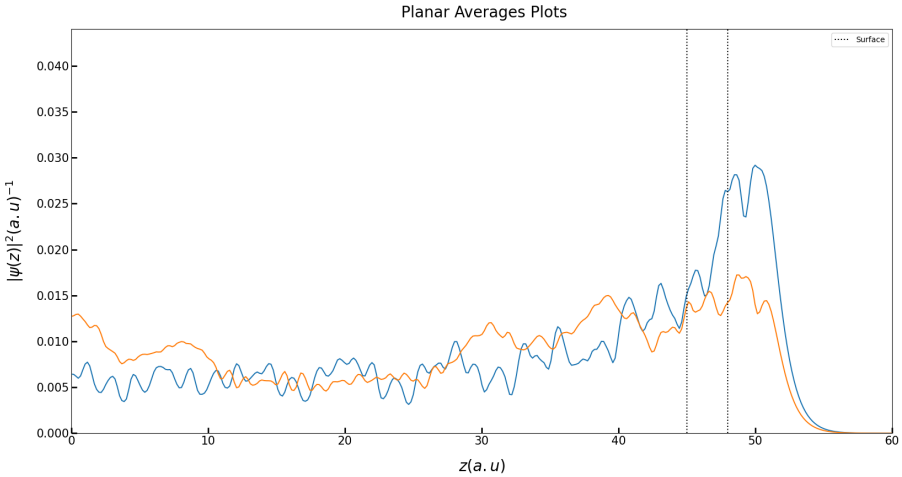

(a)

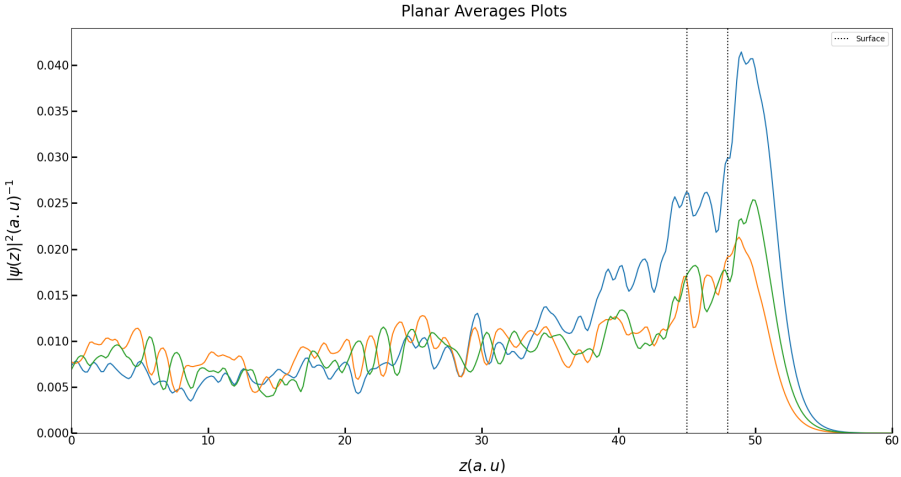

(b)

Figure (8) Some of he planar average of the surface states shown by the arrow at (a) -0.375 eV and (b) -0.121 eV

can be attributed to the fact that the Au(322) surface is not highly localized like the rest, instead, it is surface modulated, where the wave function is free to move from one step to another. In other words, the potential barrier is not higher than the kinetic energy of the effective electronic state, and thus

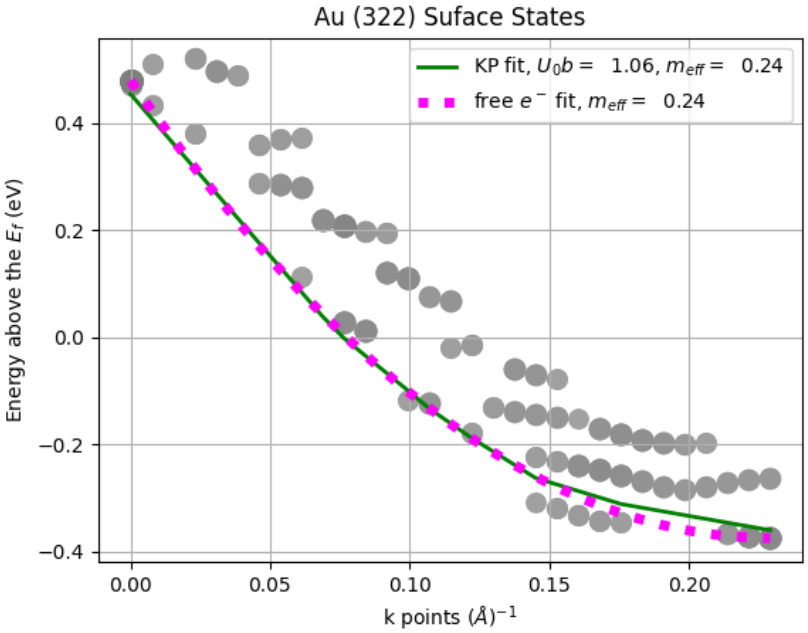

Figure (9) The potential of the Kronig penny can be modeled as a series of delta functions

electron can propagate across the barrier like a free electron. We will not see this behavior in wider surfaces where the states are terrace-modulated. If you continue the Au(322) bands to the higher unoccupied states you will find that KP can do fits that the free electron model cannot.

3.2: Au (788) Vicinal Surface

Let's now focus on the Au(788)vicinal surface, specifically at the miscut angle $\alpha = 3.5°$. Previous observations [35, 42, 48] indicate that the surface state exhibits weakly dispersing bands characteristic of a 1D quantum well. In Fig. 5.13, I present a portion of the ab initio band structure, highlighting the surface band dispersion along the $\bar{Y}$ to$\bar{\Gamma}$ path with blue dots. Experimental data extracted from Ref. [48], marked with red points and lines, is also displayed. Similar to the findings in Ref. [48], I identified several dispersive subbands indicative of the quantum well. As observed for Au(322), there is some agreement between calculations and experiments, even without the Spin-Orbit coupling. I presume the Spin-orbit will not only shift the data points but also split the bands more clearly like in experimental

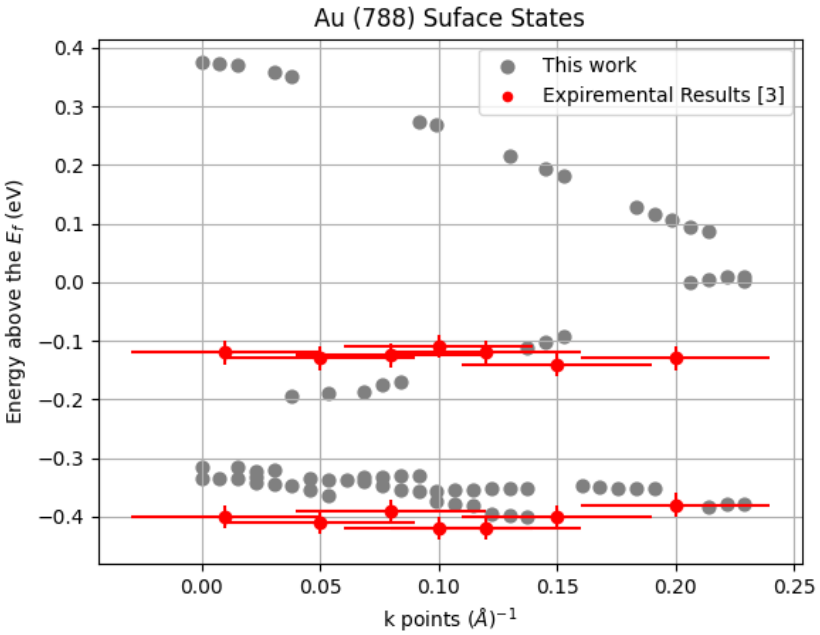

Figure (10) The potential of the Kronig penny can be modeled as a series of delta functions

results. This shift is consistent with the influence of spin-orbit coupling, a factor neglected in this calculation.

Let's delve into the localization and characteristics of the surface state at various points in the surface Brillouin zone (SBZ). Fig. 5.14 displays the planar average for the first subband bottom at $\bar{Y}$, maximum at $\bar{\Gamma}$, and the second subband maximum at Y. Examining the first subband bottom at $\bar{Y}$ reveals a surface state that, while well-localized at the surface, exhibits a bulk tail typical of a surface resonance. This is attributed to the state's potential mixing with bulk states near the SBZ surface edge. Conversely, at the center of the SBZ, where a well-defined gap exists in the projected bulk states (PBS), the surface state charge density planar average resembles that of the surface state of the Au(111) surface. Similar to Au(111) and Au(322), this surface state predominantly projects onto the p atomic orbitals of the surface atoms (Table 5.2). Notably, at $\bar{\Gamma}$, 69% of the surface state projects onto the two topmost surface layers, akin to the Shockley state of the Au(111) surface. In contrast, the surface resonance at Y is only partially localized, with 65% projecting onto the three topmost surface layers.

Similar to the analysis conducted for the Au(322) surface, the 1D KP model is employed to analyze the surface band dispersion and estimate the barrier strength. Utilizing $U_0 b = 2.1eV$ and $m_{eff} = 0.25me$, the band dispersion in Fig. 5.16 demonstrates qualitative agreement between ab initio and model calculations. Both cases exhibit split bands indicative of weakly dispersive subbands in a 1D periodic potential. However, a slight upward shift of 0.04 eV in the maxima of the first and second subbands in ab initio calculations suggests that the effective mass m_{eff} obtained by the parabolic fit in the y direction might be higher than the actual value. Alternatively, it hints that the simple 1D KP model may require modification in this instance.

3.3: Au (455) Vicinal Surface

In this section, I explore the intermediate scenario between narrow and wide terraces represented by Au(322) and Au(788) surfaces, respectively. Specifically, I focus on the Au(455) surface with a miscut angle $\alpha = 5.77°$, a small enough angle to exhibit a band gap opening at the $\bar{\Gamma}$ point, and an average terrace width of $L = 23.5$ $\mathring{A}$. This terrace width ensures predominantly 2D characteristics for the surface state. Unfortunately, experimental data for Au(455) is unavailable due to potential reconstruction and faceting [1]. Commencing with the surface band dispersion along the $\bar{Y}$ - $\bar{\Gamma}$ path in Fig, I juxtapose the calculated bands with results from the 1D KP model, which will be discussed later in this section. The figure illustrates that the

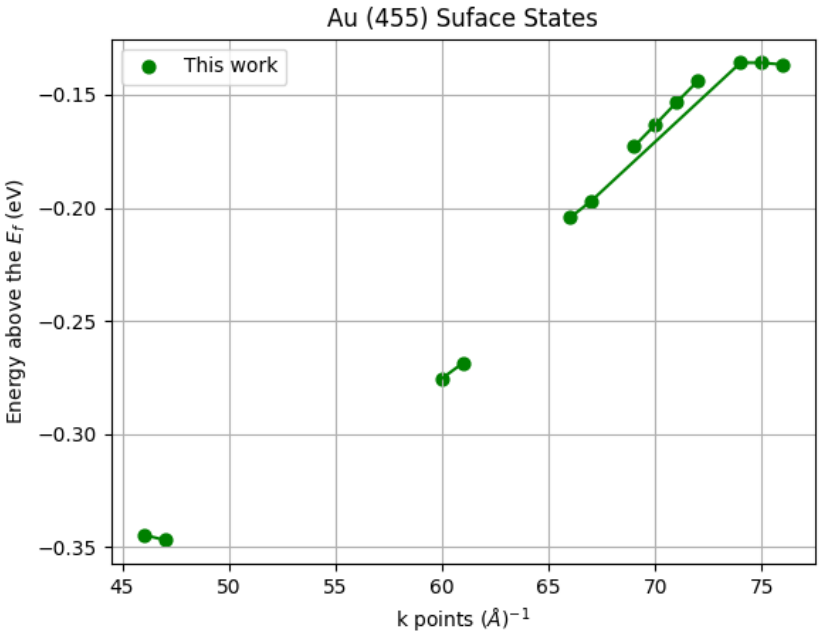

Figure (11) The potential of the Kronig penny can be modeled as a series of delta functions

Au(455) surface represents an intermediate case in terms of surface band dispersion compared to Au(322) and Au(788): the surface state is split into subbands, yet its dispersion is not as weak as that of the first subband in Au(788).

Examining the localization of the surface state in Fig. 5.18 reveals similarities to previous results in Fig. 5.14. At the bottom of the first subband at the $\bar{Y}$ point, the surface state exhibits a bulk tail in the wavefunction due to mixing with bulk states at the SBZ edges. Conversely, at the top of the first subband at the $\bar{\Gamma}$ point, where a gap exists in the projected bulk states (PBS), the surface state transforms into a true gap surface state resembling the Shockley state of the Au(111) surface. However, the in-plane behavior of the surface state wavefunction and its decay into the bulk differ qualitatively from the behavior of the Au(788) surface state shown in Fig. 5.15. At the $\bar{Y}$ point, the Au(455) surface state behaves like a 2D average-surface modulated state, extending beyond the terrace and decaying approximately in the [455] direction. While at $\bar{\Gamma}$, the state appears confined within the terrace but still senses the average surface as it decays between [455] and [111], unlike the Au(788) surface state at $\bar{\Gamma}$ shown in Fig. 5.15(b), which decays in the [111] direction. This behavior is confirmed with Eq. (5.1), where $G_m = 0.675 a.u.^{-1}$, approaching the value for a terrace-modulated state (see Table 5.1). Notably, these two values are closer to each other compared to those of the Au(322) surface, indicating that the character of the Au(455) surface lies somewhere between the terrace-modulated and average surface-modulated states.

Concluding this discussion, I briefly address the fit of the calculated bands with the KP model. The solid red line in Fig. 5.17 represents the results of the KP model calculation for the band dispersion in Au(455), utilizing a barrier strength of $U_0 b = 1.8eV$ and an effective mass $m_{eff} = 0.25me$ obtained through a parabolic fit of band dispersion in the y direction. The solid black line corresponds to the free electron dispersion. Similar to the case of Au(788), it is noted that while the minima of subbands are well reproduced with the simple model, the maximum of the band at $\bar{\Gamma}$ in the ab initio calculation is shifted up, suggesting that the effective mass is smaller than that of the flat Au(111) surface.

4. Conclusion

5. Appendices

5.1: A1

Any surface states found in these projections would be interacting with these

bulk states and hence be called resonances. Only states that are found outside of these projections are true surface states. In the Au(111) example, we see in Figure 4, the projected band structure is the yellow highlighted section in the back. It's calculated from bulk gold in the rhombohedral unit cell.

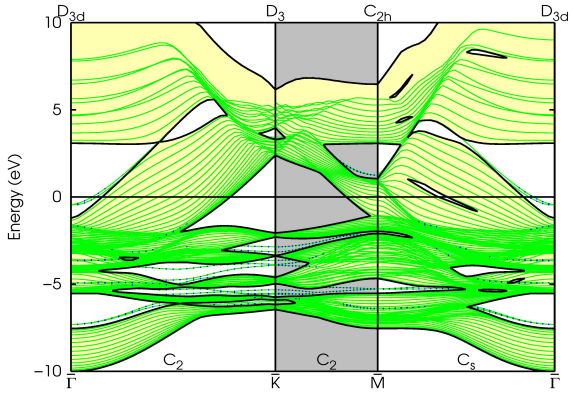

Figure (12) Au111 surface states

5.2: A2 How to construct Surface Brillouin Zone

5.3: A3 Results for projected Band structure

5.4: A4 Identifying surface states

wave functions and Shockley state identification

References

[1] A Mugarza and J E Ortega. Electronic states at vicinal surfaces. Journal of Physics: Condensed Matter, 15(47):S3281, November 2003.

[2] Riccardo Mazzarello, Andrea Dal Corso, and Erio Tosatti. Spin-orbit modifications and splittings of deep surface states on clean Au(111). Surface Science, 602(4):893–905, February 2008.

[3] A. Mugarza and J. E. Ortega. Electronic states at vicinal surfaces. Journal of Physics: Condensed Matter, 15(47):S3281, November 2003.

[4] A. Mugarza, F. Schiller, J. Kuntze, J. Cordón, M. Ruiz-Osés, and J. E. Ortega. Modelling nanostructures with vicinal surfaces. Journal of Physics: Condensed Matter, 18(13):S27, March 2006.

[5] G. Nicolay, F. Reinert, S. Hüfner, and P. Blaha. Spin-orbit splitting of the L-gap surface state on Au(111) and Ag(111). Physical Review B, 65(3):033407, December 2001. Publisher: American Physical Society.

[6] M. Šob, L. G. Wang, and V. Vitek. Local stability of higher-energy phases in metallic materials and its relation to the structure of extended defects. Computational Materials Science, 8(1):100–106, May 1997.